**Title**

A MOLECULAR BEAM SURFACE SCATTERING STUDY OF AMMONIA OXIDATION ON THE Pt(lll) CRYSTAL FACE

**Permalink**

https://escholarship.org/uc/item/6681v7fk

**Author**

Asscher, M.

**Publication Date**

1983-10-01

**Lawrence Berkeley Laboratory**
UNIVERSITY OF CALIFORNIA

## Materials & Molecular Research Division

Submitted to the Journal of Physical Chemistry

# A MOLECULAR BEAM SURFACE SCATTERING STUDY OF AMMONIA OXIDATION ON THE Pt(111) CRYSTAL FACE

M. Asscher, W.L. Guthrie, T.-H. Lin, and
G.A. Somorjai

October 1983

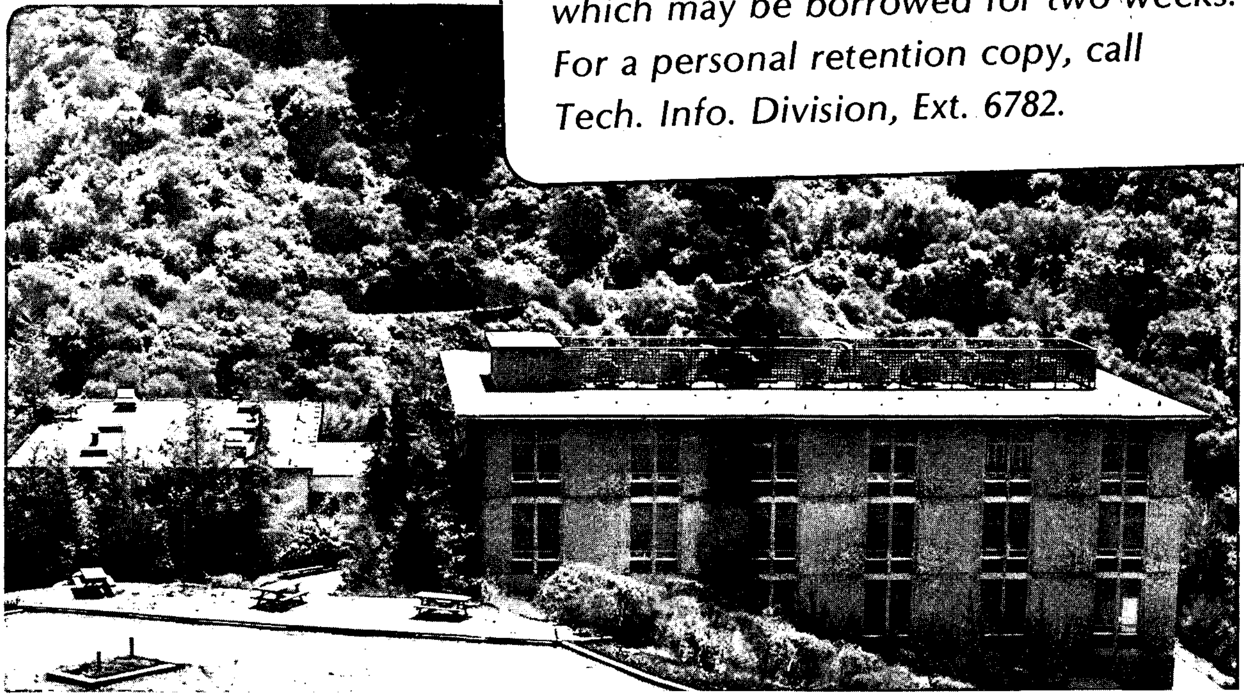

Prepared for the U.S. Department of Energy under Contract DE-AC03-76SF00098

LBL-16353

# A MOLECULAR BEAM SURFACE SCATTERING STUDY OF AMMONIA OXIDATION ON THE Pt(111) CRYSTAL FACE

M. Asscher, W. L. Guthrie, T. -H. Lin and G. A. Somorjai

Materials and Molecular Research Division,
Lawrence Berkeley Laboratory and
Department of Chemistry
University of California, Berkeley
Berkeley, California 94720, USA

# A Molecular Beam Surface Scattering Study of Ammonia Oxidation on the Pt(111) Crystal Face

By M. Asscher, T. -H. Lin, W. L. Guthrie, and G. A. Somorjai

Materials and Molecular Research Division, Lawrence Berkeley Laboratory
and
Department of Chemistry, University of California, Berkeley, CA 94720

## Abstract

The catalyzed reaction of ammonia and molecular oxygen on a Pt(111) single crystal surface was studied over the crystal temperature range of 550-1100K. A molecular beam-surface scattering technique was utilized and two-photon ionization was used to probe the NO product. Two different NO production kinetics were observed. These could be characterized by activation energies of 29 ± 4 kcal/mole, and 14 ± 3 kcal/mole for the faster and slower processes respectively. The internal energy distributions of the scattered NO product, e.g. rotational and vibrational energies, were found to have a lower temperature than the crystal temperature. Possible reaction mechanisms are discussed.

## 1. INTRODUCTION

The oxidation of ammonia to NO and $H_2O$ is one of the most exothermic chemical reactions. It is catalyzed by platinum and its alloys and is important in the chemical industry for the production of nitric acid. The kinetics of this reaction over platinum and other nobel metals has been studied by several groups over the years (1-4). These studies were conducted at pressures in the range of $10^{-3}$ - 1 torr under steady state conditions, but without attempting to characterize the metal catalyst surfaces (1-3). Surface studies under ultrahigh vacuum conditions and well defined stepped Pt catalyst were also reported (4). A surface reaction among the adsorbed reaction intermediates is thought to be the rate limiting step (Langmuir-Hinshelwood mechanism) (3), yet details of the elementary reaction steps, the nature of the reaction intermediates and their role in the reaction mechanism have not been determined.

Reactive molecular beam-surface scattering studies are well suited for exploration of the elementary reaction steps and energy transfer between the catalyst surface and the reactant during this exothermic reaction. We used molecular beams of $NH_3$ and $O_2$ and the well characterized (111) crystal face of Pt to study this reaction in the temperature range 550-1100K. The reaction probability on a single collision could be determined this way along with the activation energies of the various surface processes. The internal energy content of the scattered NO product, e.g. rotational and vibrational, has been determined using a laser resonant two photon ionization technique. We found that at least two different mechanisms for the production of NO coexist and could be characterized by different kinetic parameters 29 ± 4 and 14 ± 3 kcal/mole activation energies were found for the faster and slower mechanisms respectively. The internal states' distributions of rotational and vibrational levels are characterized by temperatures lower than the crystal temperature.

## 2. EXPERIMENTAL

For the experiment described below two separate supersonic molecular beams were used: a continuous $O_2$ beam and a $10H_z$ chopped $NH_3$ beam. These beams intersect at the center of the Pt(111) single crystal surface which is maintained under the UHV conditions. The NO product is monitored via a resonant two-photon ionization process using a tuneable UV laser. The $NO^+$ ions are collected and the current is amplified by an electron multiplier.

The molecular beam-surface scattering apparatus was described previously (6) and the modifications necessary to enable lazser two-photon ionization detection were given in detail elsewhere (7). Here we shall focus on the details pertinent to the reactive scattering study. The $NH_3$ and $O_2$ nozzles were typically operated at 140 and 160 torr backing pressure respectively.

The NO molecules were detected in the plane of motion of the laser beam focal point, which was adjusted to correspond to the plane defined by the ammonia beam and the surface normal. The incident $NH_3$ beam is typically 52° or 64° from the crystal surface normal. The $O_2$ beam is 29° from the plane of detection. The nozzles are 0.075mm in diameter and the beams are 1.5mm in diameter at the Pt(111) sample center. Each beam is estimated to have a molecular flux at the crystal surface of ca. $10^{15}cm^{-2}sec^{-1}$. No information was available on the translational and internal energy of the incident molecules.

A $10H_z$ chopper was attached to the $NH_3$ source. A continuously variable delay box (PAR 162 boxcar integrator, time scan mode) triggered by an optical trigger attached to the chopper controlled the laser pulse timing. The $NH_3$ beam pulse duration at $10H_z$ was 5msec with a rise time of ca. 0.25msec. The incident pulse shape was monitored by two photon ionization of a pure NO beam, scanning the ionizing laser pulses in time along the incident molecular pulse. This is done while the Pt(111) crystal is removed from the molecular beam path. The same technique is used to follow the production kinetics of the NO while the $O_2$ and $NH_3$ beams impinge on the Pt(111) single crystal surface, with the laser beam directed at the scattering angle of maximum NO signal, i.e., normal to the surface. Rotational state selected angular distributions of the desorbed NO product are achieved by tuning the laser frequency to a given rovibronic transition of the NO molecules, and collecting the generated ions as a function of the scattering angle (7). Rotational state distributions of NO molecules are detected by scanning the UV wavelength in the 226 or 236 nm range, where one photon resonances of the $A^2\Sigma^+(v'=0,j') \leftarrow X^2\Pi_{1/2}(v''=0,1;j'')$ rovibronic transitions lead to ionization by the absorption of a second photon of the same frequency. Vibrational excitation in the NO product was monitored as well, details of this measurement are explained elsewhere (7). The ions in these measurements are collected by a Cu-Be electron multiplier (Hamamatsu R-595) typically operated at bias voltages of 3000-4000 volts, with a gain of ca. $10^5$-$10^6$.

The laser system consists of a commercial Quanty Ray Nd:YAG pumped dye laser together with a wavelength extention unit. This laser system generates tunable UV radiation with energies of 0.7-1.0 mJ/pulse in the 226 and 236 nm range. The laser line width was ca. 2 $cm^{-1}$(FWHM). Laser frequency tuning, pulse energy and $NO^+$ ion currents were controlled, monitored and averaged by means of a NOVA 2 Computer (7).

The UHV system had a base pressure of $(4 \pm 1) \cdot 10^{-10}$ torr, but when both the $O_2$ and the $NH_3$ beams were on the pressure rose to $3 \cdot 10^{-9}$ torr. The Pt(111) sample was a disc of 0.7 cm diameter and 0.3 mm thickness. The crystal was heated by electron bombardment and its temperature was monitored by a Pt/Pt 10% Rh thermocouple spot welded to the crystal. Auger electron spectroscopy with a retarding field analyzer was used to determine the crystal cleanliness. The crystal was cleaned by an $Ar^+$ ion sputtering gun with the crystal at room temperature, followed by annealing at 800K for 2 minutes.

## 3. RESULTS

The ammonia oxidation reaction is known to produce predominantly NO and $H_2O$ over Pt catalysts at temperatures above 700K and in excess of $O_2$. Thus the reaction can be formally written as:

$$NH_3 + O_2 \xrightarrow{Pt} NO + H_2O \qquad [1]$$

We have found that under our experimental conditions about 8 ± 2% of the incident $NH_3$ is converted to NO. This value is achieved with an excess of oxygen on the surface, due to the use of a continuous $O_2$ beam and a $10H_z$ pulsed $NH_3$ beam.

### 3.1 Production Rates

In Figure 1 the ground state NO(v"=0) yield of reaction [1] as a function of the Pt(111) crystal temperature is presented as filled circles on a dashed line. Here the laser frequency is tuned to match the band head of the $P_{21}+Q_{11}$ rovibronic branch in the $A^2\Sigma^+(v''=0) \leftarrow X^2\Pi_{1/2}(v''=0)$ electronic transition of the NO molecule, where rotational levels $J''=(1/2)-7(1/2)$ are excited. These data points represent reaction conditions in which the $O_2$ nozzle operates continuously while the $NH_3$ beam is chopped at $10H_z$. There is a clear maximum of the production rate of NO at about 800K. The NO production starts around 550K and drops sharply above 850K. A continuous $NH_3$ beam source has been used as well as shown by open circles on a solid line. Under these conditions the concentration of the nitrogen containing species increases, possibly due to the increased surface concentration of ammonia fragments. There is a slight increase in the temperature of maximum NO production rate and an overall broadening of the temperature range in which NO is produced.

In order to follow the reaction kinetics, the laser pulses were delayed continuously in time compared with the incident $NH_3$ beam pulse as shown in Figure 2. The delay range was typically -5 to +50 msec relative to the onset of the 5 msec wide $NH_3$ beam pusle. The evolution of ground state NO product was found to be fairly slow even at crystal temperatures as high as 800K. Two different mechanisms of NO production were found, characterized by a fast rate with high activation energy and a slower rate with smaller activation energy. In all these curves there is a steady state background that does not decay during the time between successive $NH_3$ pulses (100 msec). This background varies from 20% of the maximum at 720K to 10% at 870K. When the $NH_3$ beam was blocked there was no detectable NO signal. At the top of Figure 2 the incident $NH_3$ pulse shape is shown. This was recorded by having NO molecules in the source chamber, monitoring the incident beam shape by intersecting the laser beam with the incident molecular beam and sweeping the laser pulse in time.

Arrhenius plots of the pseudo first-order NO production rates versus inverse of the crystal temperature for the two mechanisms are shown in Figure 3. At temperatures above 840K the time response of the fast mechanism is faster than the fall off of the incident $NH_3$ beam pulse, therefore data points of this mechanism are limited to temperatures lower than 840K. The activation energy for the faster mechanism is 29 ± 3 kcal/mole while for the slower mechanism an activation energy of 14 ± 3 kcal/mole is found.

### 3.2 Reactants Flux

Varying the stagnation pressure of the $NH_3$ or the $O_2$ beams, e.g. changing the flux on the surface, had an effect on the relative weight of the two mechanisms observed. In Figure 4 the time dependent NO production is shown for three conditions at crystal temeprature of 740K: a) Stagnation pressure of $O_2$ is reduced by a factor of 5 (the exact change of the flux on the surface could not be measured), where the importance of the fast mechanism is clearly reduced. b) Backing pressure of $NH_3$ is reduced by a factor of 7 (again the exact reduction in flux on the surface is unknown). Here the fast mechanism dominates the overall production of NO. c) Finally the ordinary conditions in which the stagnation pressures are 160 and 140 torr for $O_2$ and $NH_3$ beams respectively. The relative contributions of the two mechanisms is an intermediate between cases a and b.

### 3.3 Angular and Internal States Distributions

In order to gain some insight into the dynamics of the final step of the NO production, an angular distribution of the NO(v"=0) product was measured. In Figure 5 the angular distribution of NO is shown for a crystal temperature of 804K and $NH_3$ incident beam angle of 64°. The experimental distribution can be fitted to a $\cos^{3/2}\theta_f$ function (dashed line), where $\theta_f$ is the angle of the scattered molecules from the normal to the surface.

The overall exothermicity of the ammonia oxidation reaction, e.g. the conversion of ammonia and oxygen to nitric oxide and water, is 53 kcal per mole of $NH_3$. It is interesting to determine whether any of this exothermicity can be found within the internal states of the NO product, following the surface catalyzed reaction. In order to address this question the rotational and vibrational distributions were measured at the temperature of maximum NO production rate - 804K. The experimental details of these measurements were discussed elsewhere (7). The rotational distribution of ground state NO molecules as measured at an angle normal to the crystal surface was found to be at equilibrium with a rotational temperature of 340 ± 60K. The vibrational temperature as deduced from the vibrational population ratio of $NO(v''=1)/NO(v''=0)$ (7) was 660 ± 70K.

## 4. DISCUSSION

A conversion yield of ca. 8% of $NH_3$ to NO that was found in this study is far lower than the industrial yield of up to 95-99%. It is not surprising, however, in view of the low effective pressure of the two reactants under our reaction conditions (ca. $10^{-5}$ torr). Moreover, the (111) face of Pt single crystal is not the most effective structure to catalyze this reaction. Steps sites were found to be important (4) and more active than the (111) face by at least a factor of 4 (11b).

### 4.1 Reaction Mechanisms

The use of transient kinetic measurements rather than a steady state provides the advantage of a direct observation at the reaction rates under investigation. If we assume that due to the relatively low conversion yield, the oxygen coverage is constant within 10% accuracy, then the decay curves can be analyzed as pseudo first order rates.

Under the reaction conditions of this study, there are only relatively few possible stable adsorbed species on the Pt(111) crystal surface. The oxygen molecule is known to dissociatively adsorb on Pt above 150K (9,12) with sticking probability of less than 0.025 at crystal temperatures above 600K (10). The associative desorption rate of the oxygen adatoms is coverage dependent, and a peak at 800K corresponds to an initial coverage of ca. 1/2 max, which is estimated to be 0.25 of a monolayer (10,12). The NO production profile as a function of the Pt(111) crystal temperature is similar to the thermal desorption of $O_2$ from clean Pt(111) (Figure 1). The shift in the maximum production rate to higher temperature when a continuous $NH_3$ beam is used reflects an increase in the concentration of nitrogen containing species on the surface. This in turn increases the rate of the competing process, namely the production of $N_2$, thus a reduction in the NO production rate is expected. This indeed is observed near the 800K peak. But at higher temperatures the NO production is again a more favorable reaction path, therefore a shift to higher temperature is observed in the maximum production rate of NO. The discussion above implies that higher coverage of oxygen adatoms (excess oxygen over $NH_3$) would induce higher NO production rates at lower temperatures. Similar results for excess $O_2$ over $NH_3$ were reported previously (4), in a steady state, UHV study of this reaction on a stepped Pt surface. The shift of maximum NO production rate to higher temperatures at higher $NH_3$ pressures was also reported in a higher pressure study of this reaction on a polycrystalline Pt wires (3).

The exact composition of the nitrogen containing fragments on the surface is uncertain since no direct evidence exists under clean, well characterized surface conditions. In a study of the same reaction on a polycrystalline Pt foil in a fast flow experiment at reactants pressure range of 0.01-0.1 torr, however, Selwyn et al (13) reported the desorption of NH and OH radicals during the coarse of the reaction, using laser induced fluorescence. They concluded that the nitrogen containing ammonia fragments which are most likely to be stable on the Pt surface above 650K are $NH_{ad}$ and $N_{ad}$ (13). From a detailed molecular beam study of $NH_3$ on Pt(111) (11), a decomposition onset above 600K was reported, which is very close to the onset of the NO production. This study could not provide information on the fragments of $NH_3$ which exist on the surface above 600K. However, the coincidence of the NO production with the onset of $NH_3$ decomposition on the clean surface implies that direct reaction between O atoms and $NH_3$ molecules to produce NO are unlikely to have an important role. With the assumptions made above as to the possible adsorbed species, the following Langmuir-Hinschelwood mechanisms are suggested to occur simultaneously, and can be formally written as:

$$O_{ad} + N_{ad} \xrightarrow{k_2} NO_{ad} \xrightarrow{k_d} NO_{gas} \qquad [2]$$

$$O_{ad} + NH_{ad} \xrightarrow{k_3} NO_{ad} + OH_{ad} \xrightarrow{k_d} NO(gas) + OH_{ad} \qquad [3]$$

The assignment of the proposed processes to either the faster or the slower mechanisms (see Figure 2) can be rationalized using available thermodynamic data.

### 4.1a Slow Mechanism

The Pt-N bond energy is 14 kcal/mole (13), while the Pt-NH bond was assumed to be unstable with respect to $N_2$, $H_2$ and Pt by about 20 kcal/mole (13). At low coverages the Pt-O bond energy is about 25 kcal/mole (10), and the Pt-NO bond energy is about 28 kcal/mole (14,15). All these numbers were taken for surfaces without coadsorption of other species, therefore the validity of these numbers for the ammonia oxidation case is conditional upon having a relatively low coverage and weak interaction between the coadsorbates.

We assign reaction [2] to the slower mechanism observed experimentally with ${}^2E_a$ = 14 kcal/mole (see Figure 3). Since the $N_{ad}$ species are more stable than the $NH_{ad}$ fragments, it is likely to observe higher concentration of $N_{ad}$ than of the $NH_{ad}$ species tens of milliseconds after the termination of the incident $NH_3$ pulse. The large discrepancy between the observed (14 kcal/mole) and the calculated (32 kcal/mole) values for the activation energy is not clear. It can be rationalized, however, by considering the oxygen coverage on the Pt(111) during the reaction. It is known that the Pt–O bond energy decreases almost 10 kcal/mole by varying the oxygen coverage from zero to saturation (17). The effect of oxygen coverage on the Pt-N bond strength had not been studied, but the trend is expected to be similar (for other adsorbatres, e.g., NO(15) and OH(18), the interaction with Pt was also shown to decrease in the presence of $O_{ad}$). We conclude therefore, that the observed value for the activation energy of the slow mechanism, of 14 kcal/mole, reflects the heat of formation of the reactants and products of mechanism [2] under our reaction conditions, e.g., coadsorption of $N_{ad}$ and $O_{ad}$, the latter at an estimated steady state coverage of ca.~0.2 θ max.

### 4.1b Fast Mechanism

In order to evaluate the kinetic parameters of the second process [3], one has to consider the Pt-NH binding energy. This bond was estimated to be unstable with respect to the elements, e.g., Pt, $H_2$ and $N_2$ by about 20 kcal/mole (13). Using this information the first step of [3] is expected to be exothermic by 26 kcal/mole. Our experimental data, however, indicate that the fast mechanism is an activated process with $E_a$=29 ± 3 kcal/mole. If the first step in mechanism [3] is the rate determining one, an activation energy of 29 kcal/mole should be associated with this step. In this case the excess energy within the NO product would be near 35 kcal/mole if the molecule remains on the surface upon formation and about 7 kcal/mole if it is emitted directly to the gas phase once it is formed. Both cases seem highly unlikely in view of the fact that the NO molecules were scattered with very small internal energy. It is suggested, therefore, that the first step of [3] is fast, and the rate determining step is the desorption of $NO_{ad}$ to the gas phase. This process is known to be endothermic by about 28 kcal/mole (14), and recently was proposed to have such desorption energy from Pt(111) if defects exist at high enough density (15). Yet in order to be consistent with the observed rates of the fast mechanism, the preexponential factor must be of the order of $10^{11}$ $sec^{-1}$. Values ranging from $10^{13}$ to $10^{16}$ $sec^{-1}$ were proposed in the literature for the NO/Pt(111) system (15-17). Our estimated value of $10^{11}$ $sec^{-1}$ is therefore too low by at least two orders of magnitude for a clean Pt(111) surface. In the ammonia oxidation case, however, the coadsorption with other species may imply a decrease of the preexponential factor as compared with the clean Pt(111) surface. Indeed the desorption kinetics of NO from an oxygen precovered Pt(111) surface was reported to have a lower preexponential than from the clean Pt(111) surface (17), although in this work the desorption energy was found to decrease significantly as well (17).

One should consider also the possibility that both mechanisms [2] and [3] suggested here, originate from mechanism [2] considering the changes in the $O_{ad}$ concentration on the surface during the reaction. The steady state $O_{ad}$ concentration is expected to decrease during the time the $NH_3$ beam is on (5 msec pulse width) due to the consumption of $O_{ad}$ by the NO and $H_2O$ production during the oxidation reaction. The lowest $O_{ad}$ concentration is reached near the termination of the $NH_3$ pulse, then it starts to recover back to the steady state concentration when the $NH_3$ pulse terminates. At this point, immediately after the $NH_3$ pulse terminates we measured our fast NO production mechanism and observed Ea=29 kcal/mole for this process. If we assume that the $O_{ad}$ coverage at this point is small, then the observed value of Ea is close to the calculated 32 kcal/mole activation energy for mechanism [2] under zero coverage conditions. At the tail of the NO production transient (Figure 2), where we measured the slow mechanism's activation energy of 14 kcal/mole, the $O_{ad}$ concentration already increased close to its steady state value which may reflect the higher $O_{ad}$ coverage conditions as discussed above. Different kinetics observed during a transient measurement of CO oxidation on Pt, were recently ascribed to transient oxygen coverage changes during the oxidation reaction (19). It is difficult to distinguish between the two possibilities for the fast mechanism using our experimental data. Some independent experiments during a transient $NH_3$ oxidation reaction that will identify fragments on the surface during the coarse of the reaction might be helpful. Nevertheless, it looks to us that reaction mechanism [3] can explain the results more consistently in view of the fact that very low $O_{ad}$ concentration would result in a slow NO production rate at the point we observed the faster rate. Moreover, from the experiments in which the flux of the $O_2$ and $NH_3$ beams were varied (Figure 4), it is clear that the fast mechanism is enhanced at high $O_2/NH_3$ ratios rather than lower ratios, as the above mechanism implies.

The decay curves shown in Figure 4 at different reactants flux are consistent with the two mechanisms proposed above. They indicate that at low oxygen coverage the fast mechanism [3] is slower, which allows other reaction pathways that are minor at high oxygen coverage, to compete more effectively with the NO production. These reactions may be dissociation of NH to $N_{ad}$ + $H_{ad}$ or reaction between two $NH_{ad}$ species to produce $N_{ad}$ or $N_2$. Under these conditions, therefore, the relative contribution of mechanism [2] is enhanced. Mechanism [3] becomes the more important pathway, if the $NH_{ad}$ concentration is smaller by reducing the incident $NH_3$ flux. Then there is an excess of oxygen over $NH_{ad}$ species and a reaction between $NH_{ad}$ species is less likely.

It is interesting to note that under higher pressure conditions on a polycrystalline Pt wire catalyst (3) an activation energy of 21.7 kcal/mole is reported for the production of NO, which is an intermediate value between the two activation energies that are reported here.

### 4.2 Angular and Internal State Distributions

Both vibrational and rotational states distributions were found to be colder than the equivalent measurements for NO scattered from a clean Pt(111) surface (7). These results imply that in both mechanism [2] and [3] the NO product remains at the surface upon formation as the first step and desorbs only after a rather long residence time. It is not surprising that the internal energy distributions of the desorbed NO from the Pt(111) surface under reaction conditions are different from those from a clean Pt(111) surface. It is unclear, however, what is the meaning of the colder distributions observed and to what extent the presence of coadsorbed oxygen atoms and N and NH fragments contribute to those observations.

The angular distribution of the NO product is slightly peaked towards the normal to the surface and varies as $\cos^{3/2}\theta_f$, $\theta_f$ being the angle from the surface normal. This may be due to corrugation of the surface, resulting from the various adsorbates. A recent study of directed desorption (20) predicts dramatic effects of corrugation near adsorption-desorption sites on the angular distribution of the desorbing molecules: the more corrugated the surface the more the angular distribution is peaked towards the surface normal (20).

## 5. CONCLUSION

We have studied the ammonia oxidation reaction on a Pt(111) single crystal surface using a molecular beam surface scattering technique with laser two-photon ionization as a probe to follow the production of NO. It was found that at lest two competing mechanisms for the production of NO molecules coexist. One mechanism is suggested to involve a surface reaction between adsorbed atomic oxygen and nitrogen, characterized by an activation energy of 14 kcal/mole. The second and faster mechanism is between oxygen and an NH fragment in which the desorption of NO is the rate limiting step. The internal state energy distributsion (e.g., vibrational and rotational states of the product), were found to be characterized by temperatures lower than the crystal temperature.

## ACKNOWLEDGEMENTS

This work was supported by the Director, Office of Energy Research, Office of Basic Energy Sciences, Materials Sciences Division of the U.S. Department of Energy under Contract Number DE-AC03-76SF00098.

We would like to acknowledge the San Francisco Laser Center for providing the laser system under NSF Grant CHE79-16250. M. Asscher would like to thank the Chaim Weizmann Post Doctoral Fellowship for providing a Post Doctoral Fellowship.

## REFERENCES

1. Y. M. Fogel, B. T. Nadykto, V. G. Rybalko, V. I. Shvachko and I.E. Korobehanskaya; Kinet. Catal., 5, 169 (1964).
2. C. W. Nutt and S. Kapur; Nature 220, 697 (1968); ibid 224, 169 (1969).
3. T. Pignet and L. D. Schmidt; J. Catalysis, 40, 212 (1975).
4. J. L. Gland and V. N. Korchak; J. Catalysis, 53, 9 (1978).
5. M. Asscher, W. L. Guthrie, T.-H. Lin and G. A. Somorjai, Phys. Rev. Lett., 49, 76 (1982).
6. S. T. Ceyer, W. J. Siekhaus and G. A. Somorjai, J. Vac. Sci. and Technol. 19, 726 (1981).
7. M. Asscher, W. L. Guthrie, T.-H. Lin and G.A. Somorjai, J. Chem. Phys., 78, 6992 (1983).
8. J. L. Gland, Surf. Sci.; 74, 327 (1978).

9. a. J. L. Gland, B. A. Sexton and G. B. Fisher; Surf. Sci., 95, 587 (1980).
   b. J. L. Gland; Surf. Sci., 93, 487 (1980).

10. C. T. Campbell, G. Ertl, H. Kuipers and J. Segner; Surf. Sci., 107, 220 (1981).

11. a) W. L. Guthrie, J. D. Sokol and G. A. Somorjai; Surf. Sci., 109, 390 (1981).
    b) W.L. Guthrie and G.A. Somorjai, unpublished results.

12. N. R. Avery; Chem. Phys. Lett., 96, 371 (1983).

13. a) G.S. Selwyn and M.C. Lin in "Lasers as Reactants and Probes in Chemistry" W.M. Jackson and A.B. Harvey eds., Howard University Press, Washington D.C. (1983).
    b) G.S. Selwyn, G.T. Fujimoto and M.C. Lin, J. Phys. Chem., 86, 760(1982).

14. T. N. Rhodin and G. Ertl, "The Nature of the Surface Chemical Bond", North Holland Publishing Company, New York, 1979, p. 324.

15. J. A. Serri, J. M. Cardillo and G. E. Becker, J. Chem Phys., 77, 2175 (1982).

16. T. -H. Lin and G. A. Somorjai; Surf. Sci., 107, 573 (1981).

17. C. T. Campbell, G. Ertl, and J. Segner; Surf. Sci., 115, 309 (1982).

18. G.T. Fujimoto, G.S. Selwyn, J.T. Kelser and M.C. Lin; J. Phys. Chem. 87 1906 (1983).

19. G.L. Haller, private communication.

20. a. D. R. Horton, W. F. Banholtzer and R. I. Masel; Surf. Sci., 116, 22 (1982).
    b. D. R. Horton and R. I. Masel; Surf. Sci., 116, 13 (1982).

## FIGURE CAPTIONS

1. Yield of NO($v''=0$) as a function of crystal temperature. The filled circles on dashed line correspond to a continuous $O_2$ beam and a 10$H_z$ chopped $NH_3$ beam. The open circles on solid line are of two continuous beams of both the $O_2$ and $NH_3$.

2. The rise and decay of the NO($v''=0$) production rate as a function of time, at different crystal temperatures. At the top, the shape of the incident ammonia beam pulse is shown.

3. Arrhenius plots for the two NO production mechanisms. Open squares correspond to the slow mechanism and open circles to the fast mechanism.

4. The rate of NO(v="0) production as a function of time for various fluxes of reactants on the surface: a) The $O_2$ beam stagnation pressure is reduced by a factor of 5 from the pressure that corresponds to a maximum flux. b) The same for the $NH_3$ beam, but the reduction is by a factor of 7. c) Both $O_2$ and $NH_3$ beams at stagnation pressures of maximum flux on the surface, e.g. 160 and 140 torr respectively.

5. Angular distribution of the NO($v''=0$) product of the ammonia oxidation on Pt(111). The incident angle $\theta_i$ of the ammonia beam is 64°, with the crystal at 804K. The dashed line is a calculated angular distribution with the function $\cos^{3/2}\theta_r$, where $\theta_r$ is the scattering angle from the surface normal.

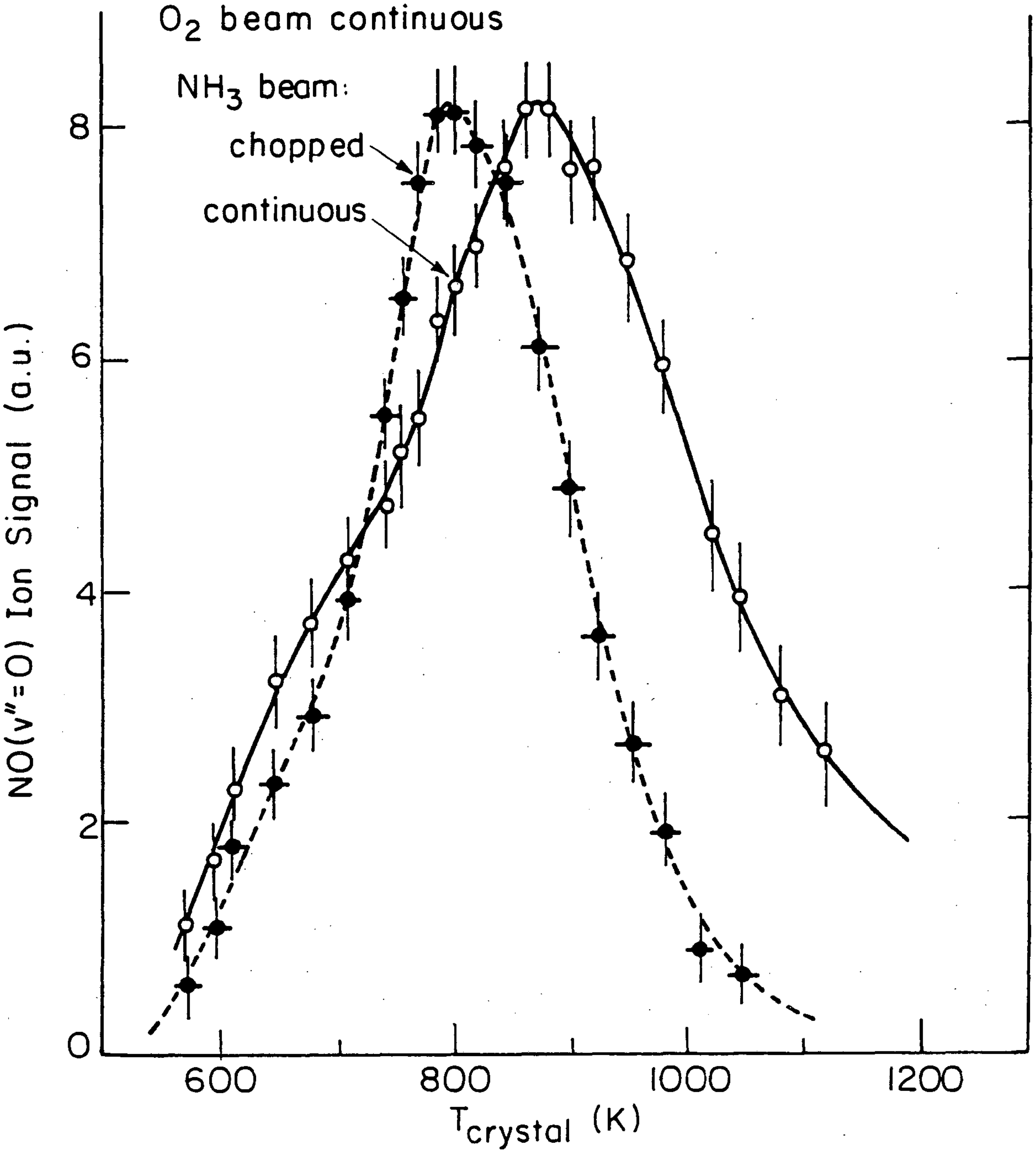
$O_2$ beam continuous
$NH_3$ beam:
chopped
continuous
NO(v"=0) Ion Signal (a.u.)
0
2
4
6
8
600
800
1000
1200
$T_{crystal}$ (K)
XBL 831-5096

Fig. 1

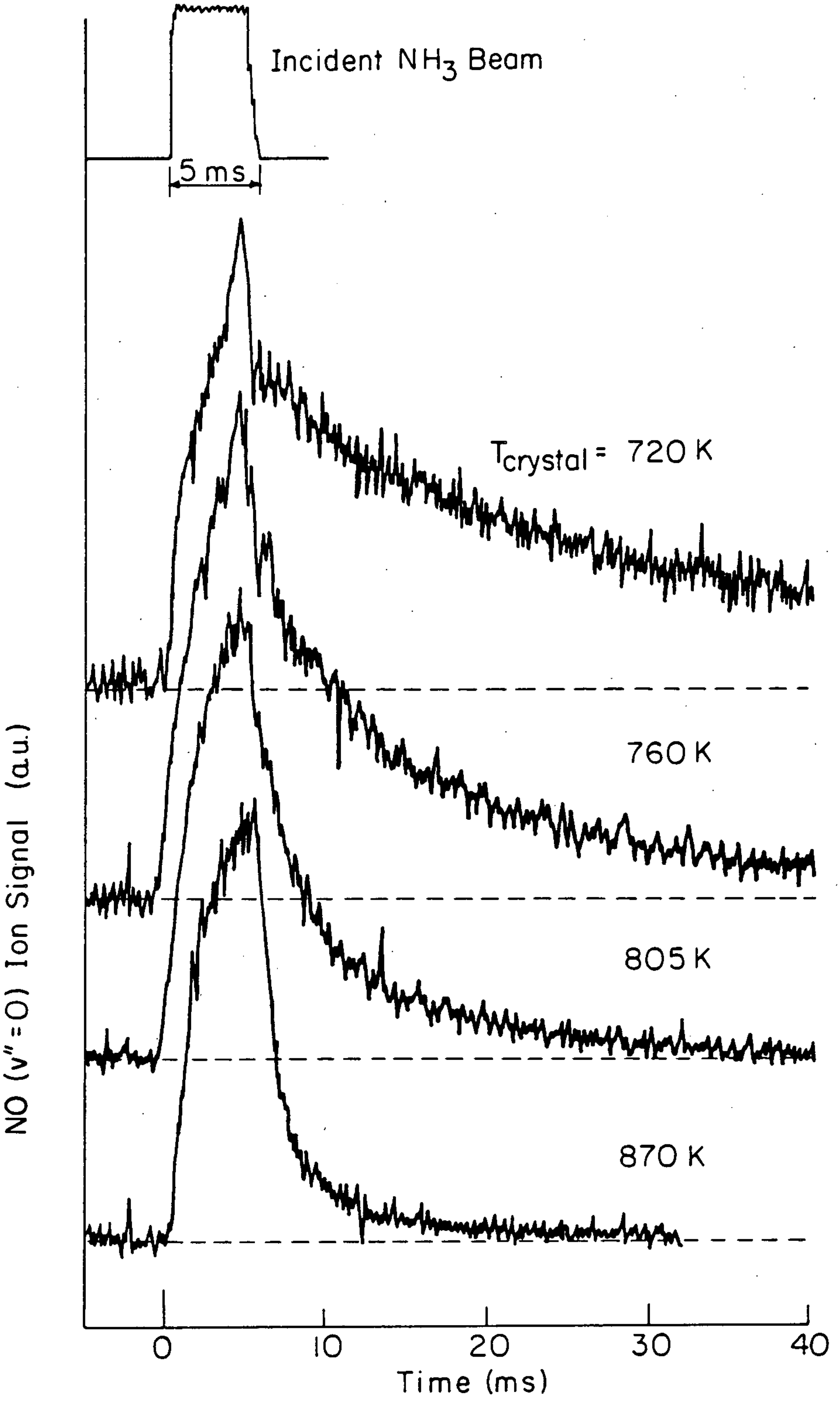

XBL 831-5094

Fig. 2

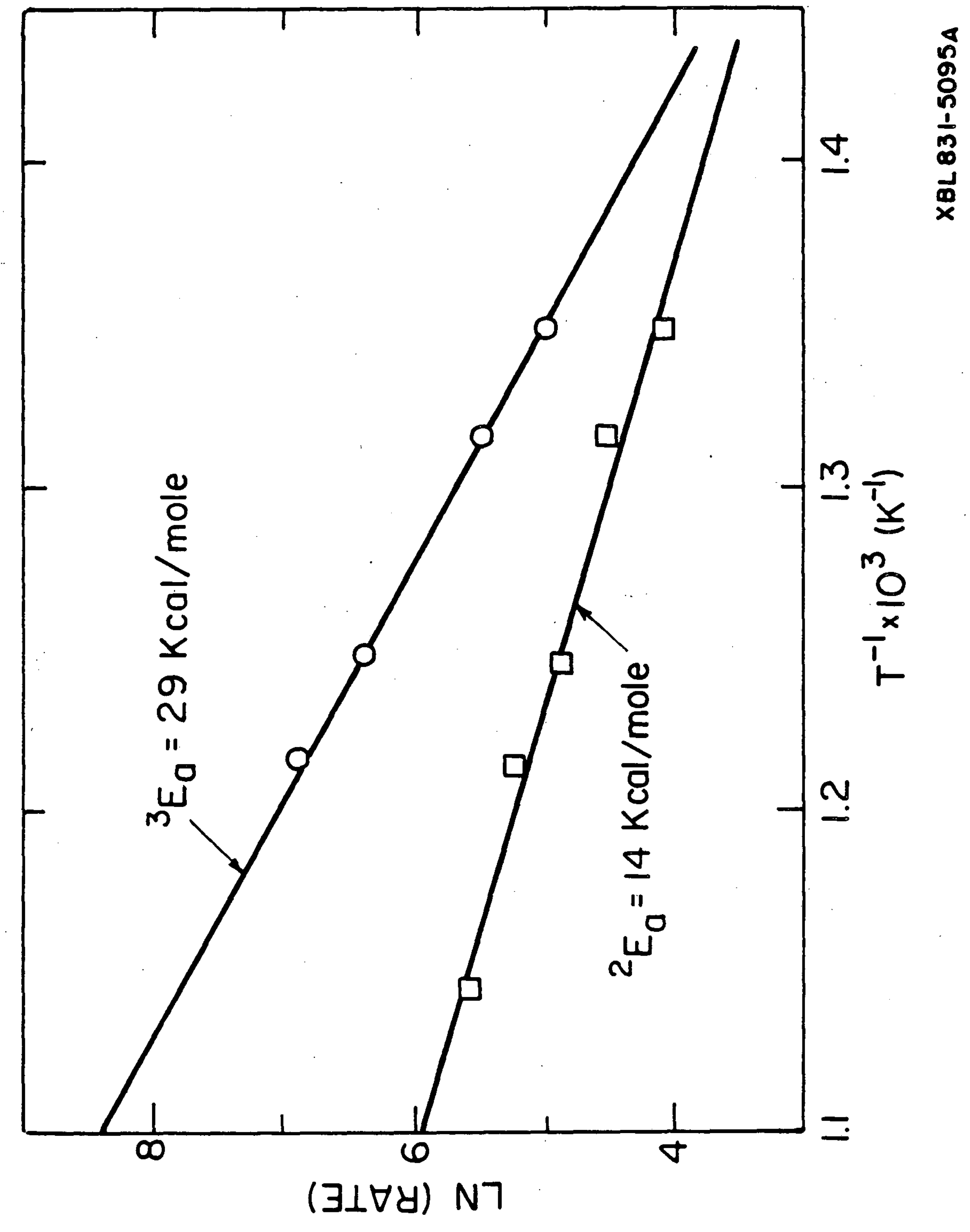
$^3E_a$ = 29 Kcal/mole
$^2E_a$ = 14 Kcal/mole
LN (RATE)
8
6
4
$T^{-1} \times 10^3$ ($K^{-1}$)
1.1
1.2
1.3
1.4
XBL 831-5095A

Fig. 3

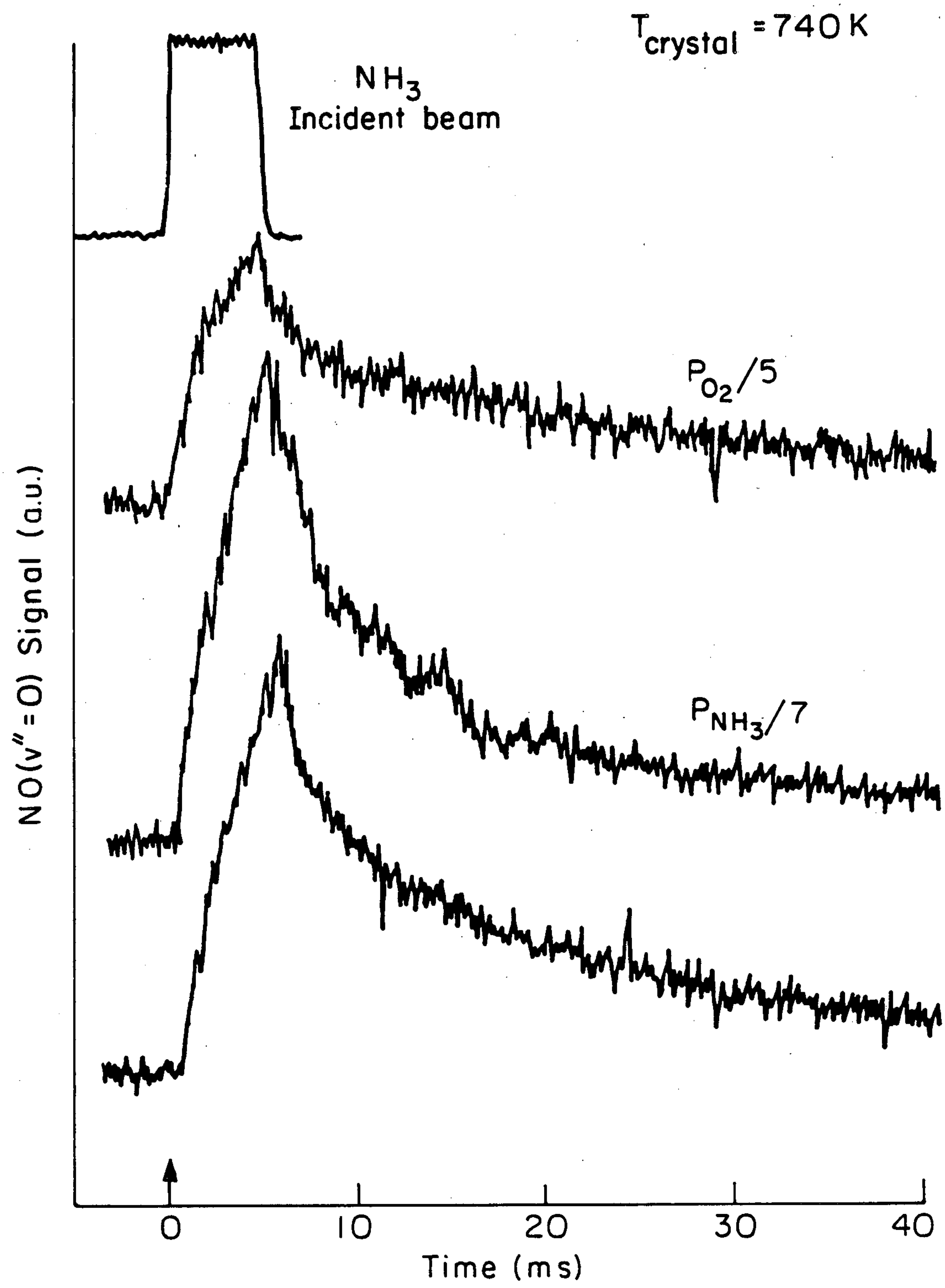

XBL 8310-6518

Fig. 4

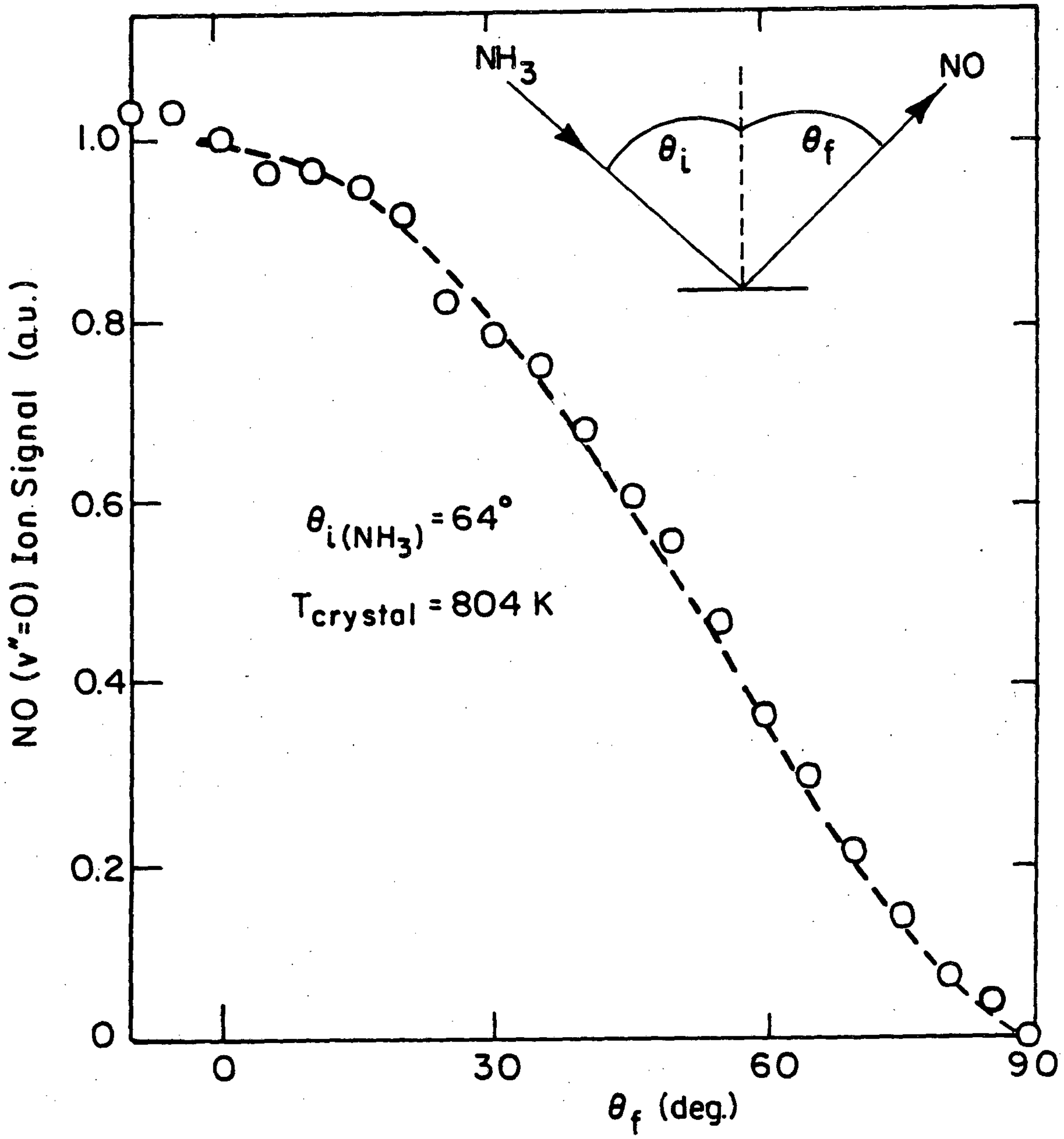

XBL 831-5093A

Fig. 5

TECHNICAL INFORMATION DEPARTMENT
LAWRENCE BERKELEY LABORATORY
UNIVERSITY OF CALIFORNIA
BERKELEY, CALIFORNIA 94720